51st AIAA Aerospace Sciences Meeting including the New Horizons Forum and Aerospace Exposition
07 - 10 January 2013, Grapevine (Dallas/Ft. Worth Region), Texas

AIAA 2013-0068

Parameter Studies on Rotational and Translational Accelerations of Flat Plates

Kenneth Granlund[1] and Michael OL[2]

U.S. Air Force Research Laboratory, Aerospace Sciences Directorate, Wright-Patterson AFB, OH 45433

Kunihiko Taira[3] and Ryan Jantzen[4]

Florida State University, Department of Mechanical Engineering, Tallahassee, FL 32310

*** This paper is submitted as an invited paper of the APA invited session: Low-Reynolds Number Aerodynamics: Modeling and Testing***

Abstract

We compare a broad range of transient translations, and a smaller collection of transient rotations, of flat plates of aspect ratio 2, 4, and nominally 2D, tracking lift and drag coefficients vs. motion history, for a range of acceleration profiles and motion modalities, and for Reynolds numbers from 14 through 10,000. Kinematics include a translational acceleration, consisting of a linear ramp in velocity vs. convective time, starting from rest and with fixed incidence angle; a pitch about various chordwise pivot points in constant free-stream; a combination of the two, with both pitch and translational acceleration; a plunging motion in steady free stream; and finally, a rotational acceleration, where the plate is again initially at rest and accelerates azimuthally to some steady rotational speed. Accelerations cover reduced frequencies from $K = \pi/48$ to $\pi/4$. Rotational and translational accelerations where studied in mixtures of glycerin and water, as well as nominally pure water, as a means of broadly varying Reynolds number. Noncirculatory loads vary as the square of the reduced frequency, and are particularly pronounced during smoothing-transients applied to linear ramps. For the cases of pitching and combined pitching and translational acceleration, moving the pitch pivot point aft delays leading edge vortex production and attenuates lift. At Re = 10,000, which was the principal Reynolds number achieved in pure water, lift and drag histories are essentially identical for the translational acceleration case. The same is true for the rotational acceleration case, implying that the net aerodynamic force is wall-normal. Further, the shape of the aerodynamic force histories is similar between translation and rotation at Re = 10,000, except that the latter has lower force peaks and lower slope of aerodynamic force vs. time, and forces continue buildup after the accelerated portion of the motion has ceased. At lower Reynolds numbers, achieved in glycerin-water mixtures, the trends in lift and drag histories are more complicated. Lift and drag histories become mutually quite different for any given case, implying that the net aerodynamic force is no longer-wall normal. And the difference between rotational and translational acceleration cases is much larger at lower Re.

Introduction

A tantalizingly basic and yet essentially intractable problem in unsteady aerodynamics is to write the history of lift, drag and pitching moment as a closed-form function of the independent kinematic variables and their first few derivatives. These would be the pitch/plunge/surge/rotation rates and accelerations. The simplicity stems from occasionally promising success of classical linear models, while the intractability is subjective judgment in what level of error from usage of such models is acceptable in complicated flows with strong vortex formation and shedding. Here we continue a series of works on the coupling between transients due to unsteady motion of a body in a flowing or quiescent fluid, and loads due to massive flow separation. Geometries remain maximally simple: rectangular flat plates of various aspect ratios, with round edges. Translationally accelerated or "surging" motion of a flat plate follows the classical problem of Wagner[1], with several differences:

1. Plate incidence angle may be high, with flow separation effects beyond the scope of Wagner's solution.
2. Smoothing of accelerations results in nontrivial motion history effects.
3. Besides the trailing-edge starting vortex, vortices are initially and then subsequently shed from the leading edge.
4. Plates of various planform require accounting of 3D effects, principally in the impact of tip-vortices on the overall vortex system.

---

[1] Post-doctoral Scholar, AIAA Senior Member
[2] Senior Aerospace Engineer, AIAA Associate Fellow
[3] Assistant Professor, AIAA Member
[4] Graduate Research Assistant, AIAA Student Member

Report Documentation Page		*Form Approved* *OMB No. 0704-0188*

Public reporting burden for the collection of information is estimated to average 1 hour per response, including the time for reviewing instructions, searching existing data sources, gathering and maintaining the data needed, and completing and reviewing the collection of information. Send comments regarding this burden estimate or any other aspect of this collection of information, including suggestions for reducing this burden, to Washington Headquarters Services, Directorate for Information Operations and Reports, 1215 Jefferson Davis Highway, Suite 1204, Arlington VA 22202-4302. Respondents should be aware that notwithstanding any other provision of law, no person shall be subject to a penalty for failing to comply with a collection of information if it does not display a currently valid OMB control number.

1. REPORT DATE **JAN 2013**	2. REPORT TYPE	3. DATES COVERED **00-00-2013 to 00-00-2013**
4. TITLE AND SUBTITLE **Parameter Studies on Rotational and Translational Accelerations of Flat Plates**		5a. CONTRACT NUMBER
		5b. GRANT NUMBER
		5c. PROGRAM ELEMENT NUMBER
6. AUTHOR(S)		5d. PROJECT NUMBER
		5e. TASK NUMBER
		5f. WORK UNIT NUMBER
7. PERFORMING ORGANIZATION NAME(S) AND ADDRESS(ES) **Florida State University,Department of Mechanical Engineering,Tallahassee,FL,32310**		8. PERFORMING ORGANIZATION REPORT NUMBER
9. SPONSORING/MONITORING AGENCY NAME(S) AND ADDRESS(ES)		10. SPONSOR/MONITOR'S ACRONYM(S)
		11. SPONSOR/MONITOR'S REPORT NUMBER(S)

12. DISTRIBUTION/AVAILABILITY STATEMENT **Approved for public release; distribution unlimited**

13. SUPPLEMENTARY NOTES

14. ABSTRACT

We compare a broad range of transient translations, and a smaller collection of transient rotations, of flat plates of aspect ratio 2, 4, and nominally 2D, tracking lift and drag coefficients vs. motion history, for a range of acceleration profiles and motion modalities, and for Reynolds numbers from 14 through 10,000. Kinematics include a translational acceleration, consisting of a linear ramp in velocity vs. convective time, starting from rest and with fixed incidence angle; a pitch about various chordwise pivot points in constant free-stream; a combination of the two, with both pitch and translational acceleration; a plunging motion in steady free stream; and finally, a rotational acceleration, where the plate is again initially at rest and accelerates azimuthally to some steady rotational speed. Accelerations cover reduced frequencies from K = $\pi/48$ to $\pi/4$. Rotational and translational accelerations where studied in mixtures of glycerin and water, as well as nominally pure water, as a means of broadly varying Reynolds number. Noncirculatory loads vary as the square of the reduced frequency, and are particularly pronounced during smoothing-transients applied to linear ramps. For the cases of pitching and combined pitching and translational acceleration, moving the pitch pivot point aft delays leading edge vortex production and attenuates lift. At Re = 10,000, which was the principal Reynolds number achieved in pure water, lift and drag histories are essentially identical for the translational acceleration case. The same is true for the rotational acceleration case, implying that the net aerodynamic force is wall-normal. Further, the shape of the aerodynamic force histories is similar between translation and rotation at Re = 10,000, except that the latter has lower force peaks and lower slope of aerodynamic force vs. time, and forces continue buildup after the accelerated portion of the motion has ceased. At lower Reynolds numbers, achieved in glycerin-water mixtures, the trends in lift and drag histories are more complicated. Lift and drag histories become mutually quite different for any given case, implying that the net aerodynamic force is no longer-wall normal. And the difference between rotational and translational acceleration cases is much larger at lower Re.

15. SUBJECT TERMS					
16. SECURITY CLASSIFICATION OF:			17. LIMITATION OF ABSTRACT	18. NUMBER OF PAGES	19a. NAME OF RESPONSIBLE PERSON
a. REPORT **unclassified**	b. ABSTRACT **unclassified**	c. THIS PAGE **unclassified**	**Same as Report (SAR)**	**16**	

This is all for the case of a plate at some fixed incidence angle in the lab-frame, with a non-constant speed relative to the free stream. We examine the special case of a linear ramp in the relative speed (with respect to convective time), with smoothing of acceleration at the beginning and ending of the ramp following the C^∞ function proposed by Eldredge[2]. Parameters to vary are the dimensionless rate of acceleration and the plate's incidence angle.

A complementary case is where the relative free-stream speed is constant, but the plate's incidence angle varies, in the present case also along a linear ramp with C^∞ smoothing transients at the beginning and the end; this is, in other words, a pure-pitch. Parameters to vary include the pitch rate and the degree of smoothing, the pitch pivot point, and the initial and final incidence angle. In all of the present cases, the initial incidence angle is zero. A third case is the combined linear ramp in translational relative speed and incidence angle. All three cases begin with a zero-lift condition, either because the initial incidence angle is zero, or the dynamic pressure is zero. All three conclude with the plate in steady relative translation speed, which together with the plate chord determines the reference Reynolds number; and all three conclude with some common final value for plate incidence angle, in the present study taken at θ=45°. These motions are all translational, in that both of the plate's wingtips (if the aspect ratio is finite) move at the same speed along the same trajectory.

A still further complementary set of cases involves rotation of a necessarily finite aspect ratio plate. The plate is at some constant incidence, and initially at rest with respect to the fluid. At motion onset, the plate accelerates in rotation about a fixed-point near one of its tips, reaching a steady rotation speed. The inboard wingtip scribes an arc of small radius, while the outboard scribes a larger one. The profile of rotational speed from initiation to completion of the accelerated portion of the motion is again a C^∞ smoothed linear ramp corresponding to some desired dimensionless frequency, and then continues as a rotation of constant speed.

Lentink and Dickinson[3] considered translational cases with streamwise acceleration, the corresponding rotational case, and several other variations, with the seminal conclusion that finite Rossby number in the rotational cases is eminently responsible for both the stability of Leading Edge Vortices (LEVs) and high lift. Rotational acceleration rate and Reynolds number were observed to have at most secondary import. The present work broadly agrees with the latter statement, in the sense that even large changes in Reynolds number manifest themselves much more in plate-axial than plate-normal loads, and that acceleration transients attenuate after 1-2 convective times. Yet there is emerging a disagreement on the importance of distinction between rotational and translational motion, as evinced in the present work and in other recent work such as that of DeVoria[4] and Jones and Babinsky[5]. The claim, in brief, is that rotation may be quintessentially favourable for retention of a large leading edge vortex (possibly depending on Reynolds number), but that rotation does not appear to offer advantage over translation in either lift-to-drag ratio or peak lift.

While we do not presently aspire to comprehensive reconciliation of the extant literature, the aim is to build a large parameter-library of cases using comparatively topical techniques (direct force measurement and flow visualization by dye injection) to compare translational and rotational motions, to then prompt deeper study of a few expository cases. The subject work is part of the NATO AVT-202 Task Group, "Extension of Fundamental Flow Physics for Practical MAV Aerodynamics", and as such aims towards basis for computational validation and investigation of experimental parameters such as the importance of blockage (distance from wingtip to boundary wall of vessel holding the working-fluid[6]).

Experimental Setup

Experiments were performed in the U.S. Air Force Research Laboratory Aerospace Sciences Directorate's Water Tunnel. This is a free-surface tunnel (18" wide, 24" high, 96" long test section; flow speed 3 cm/s – 45 cm/s; turbulence intensity ~ 0.5%) fitted with a three degree of freedom electric rig enabling independent control of pitch or rotation, plunge or heave, and surge or streamwise-aligned translation. This is for translational motions where the test-article is either translated or rotated about a line parallel to its spanwise direction; the latter motion we call "pitch". A modification of the setup enables rotational motion: the plate is mounted vertically underneath the two vertical plunge rods, and movement of all three linear motors pivots the mount connecting the two vertical plunge rods, producing a rotation of the plate about some point inboard of its root. More detail on the tunnel and rig operation is given in Ol et al.[7], and photographs of the experiment are in Figure 1. The present application combines our prior work on pitching plates, airfoils and wing planforms of various aspect ratios[8], and that on hovering free-to-pivot plates[9] using all three motors to produce a 1-DOF

motion (streamwise surge, constant free-stream pitch, or rotational surge) or 2-DOF motion (combined surge and pitch).

To investigate Reynolds number variations for motions in a quiescent ambient fluid, the test section of the water tunnel was fitted with an 18" wide, 24" high and 48" long Perspex tank filled with different mixtures of glycerine and water. Altering the viscosity of the fluid permits a much larger range of Reynolds number tests than changing the test article's velocity in water.
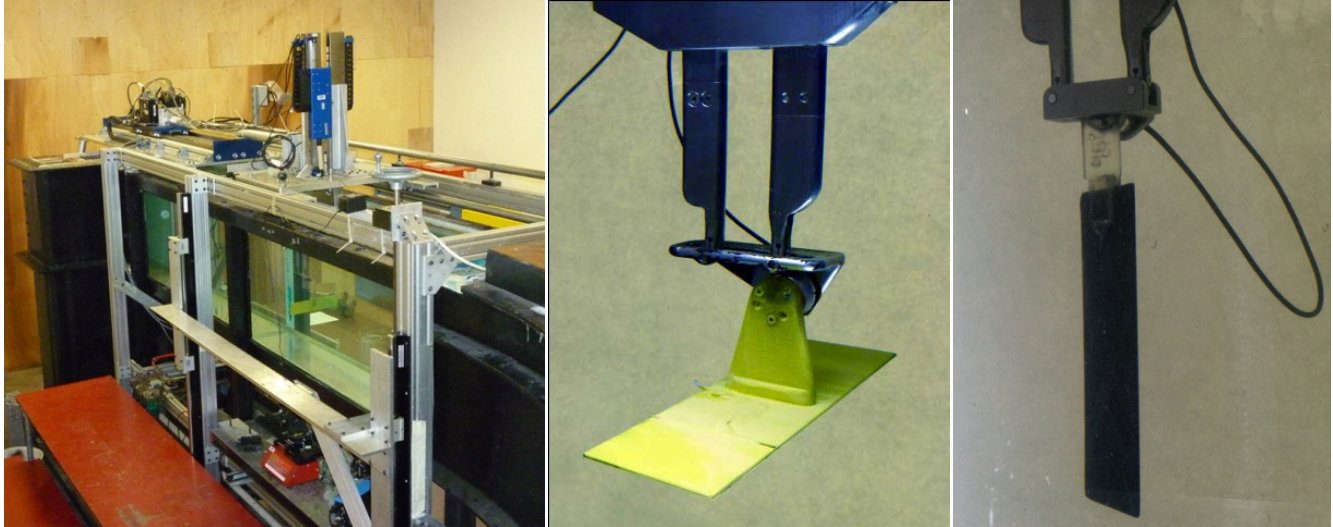
Figure 1. Experimental setup. (a) water tunnel test section, showing motion rig's linear motors above the free-surface. (b) typical flat-plate model installation (in this case, AR=4). (c) rotating-wing arrangement, with the wing hanging vertically underneath the two vertical plunge rods.

Force measurement is with an ATI Nano-17 6-component model cell, mounted on a strut on the pressure-side of the model, at its midplane. Error analysis, calibration and data processing methods are discussed by Granlund et al.[8] Flow visualization is by dye injection, typically at the ¾ span, with a dye line firing upstream at the leading edge and downstream at the trailing edge. Three plates are considered: nominally 2D, where the plate spans the test section (18" or 450mm span) with ~1mm spacing between each wingtip and its proximate test section wall; aspect ratio 4, and aspect ratio 2. The 2D and AR=4 plates had chord of 3" (~75mm), while the AR=2 plate had chord of 117mm.

Results

The selected approach for denoting motion frequency is the number of chords traveled during acceleration. The two emphasized cases are 1c and 6c in Figure 2. That is, in the faster case, if there were no smoothing transients, the translational surge would be a linear ramp in speed, from 0 initially up to the final speed, occurring over one chord length and thus having an exponential dependence on time. Smoothing transients approximate a sinusoid of amplitude of 10% of the acceleration duration. The intent is for the 1c case to emphasize fast dynamics, where the accelerated portion of the motion occurs faster than the relevant vortex-formation time scale. This is achievable in liquid-phase facilities (water, glycerin, oil); tunnels and towing tanks. The slower case is more amenable to quasi-steady approximation, and can be studied in wind tunnels as well as liquid-phase facilities. The slower case kinematics are simply a stretching in time of the faster case by factor of 6. Unless otherwise noted, results are in pure-water, at Reynolds number of 10,000 based on eventually-reached relative free-stream, and plate chord.
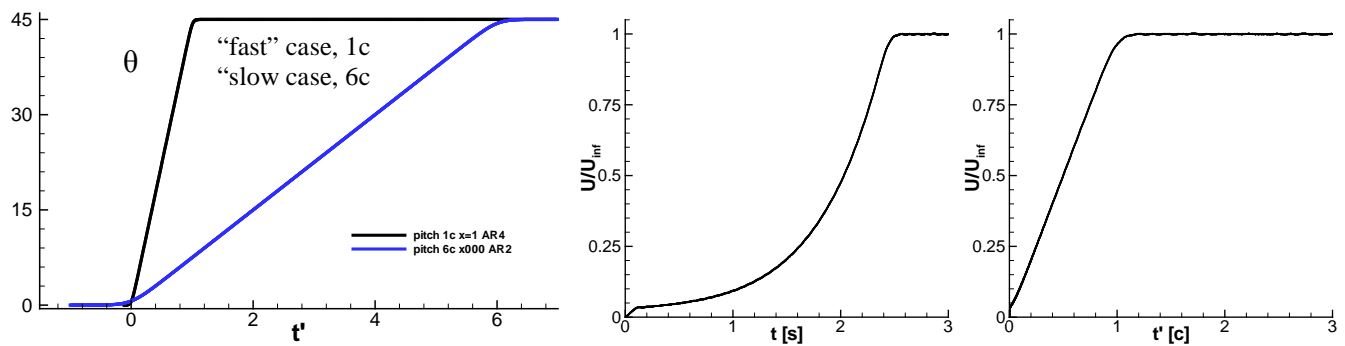
Figure 2. Motion history for the "fast" (1 chords traveled) and "slow" (6 chords traveled) cases. Left: pitch ramp, showing history of incidence angle with convective time. Middle: streamwise surge, "fast" case, showing history of normalized relative free-stream speed with respect to wall-clock or physical time; this is an exponential dependence. Right: streamwise surge, "fast case", plotted against convective time, which now becomes a smoothed linear ramp akin to the pitching case. Note that for the pitching case, θ(t) plotted vs. wall-clock or convective time is identical, because free-stream is constant. Note also the smoothing transients at t` ~ 0 and t`~1 (fast case) or t'~6 (slow case).

We begin by considering aspect ratio effects for the case of pure-pitch. Figure 3 and Figure 4 show the results in lift and drag coefficient for 6c and 1c pitching motions, respectively. The pivot point in all cases is the leading edge of the plate. For the slow case in Figure 3, increasing aspect ratio results in higher lift curve slope and higher maximum lift, occurring earlier in the motion history. After reaching an incidence angle of 45° at t'=6, the AR=4 and wall-to-wall plates produce an oscillating lift and drag, implying vortex shedding with characteristic period of several convective times, whereas the AR=2 plate does not evince shedding-type of integrated force dependency. For the fast case in Figure 4, aspect ratio increase leads to a positive offset in lift coefficient, and a very slight slope increase. The initial lift "spike" for the fast case is due to the non-circulatory contribution from the plate normal acceleration from nonzero pitch rate-of-change, colloquially denoted as "added mass". This coefficient is the same amplitude independent of aspect ratio, but the actual peak value is difficult to obtain because of nominal structural compliance and low-pass filtering of experimental force data. There is no force spike in drag at the start of the motion because the plate-normal is perpendicular to the drag axis. At the end of the pitch acceleration near t'=1, the plate is at 45° incidence angle and produces a negative spike in both lift and drag direction. For the slow case in Figure 3, the pitch rate-of-change at t'=0 and t'=6 is too low to produce discernable non-circulatory force spikes.
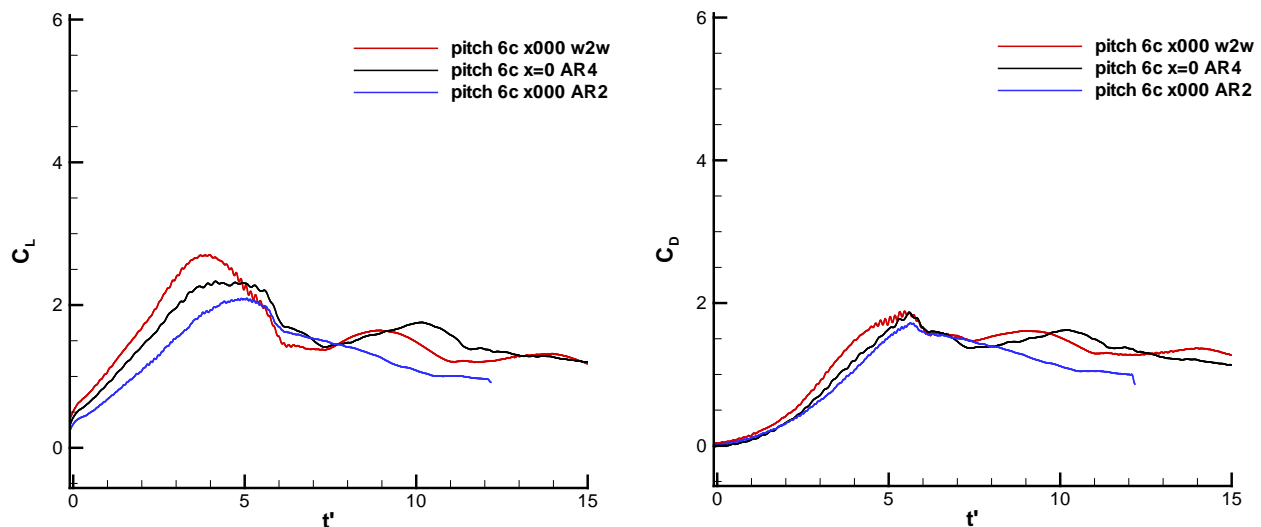

Figure 3. Aspect ratio effects on pure-pitch, pivoting about the leading edge; lift (left) and drag (right), 6c case.
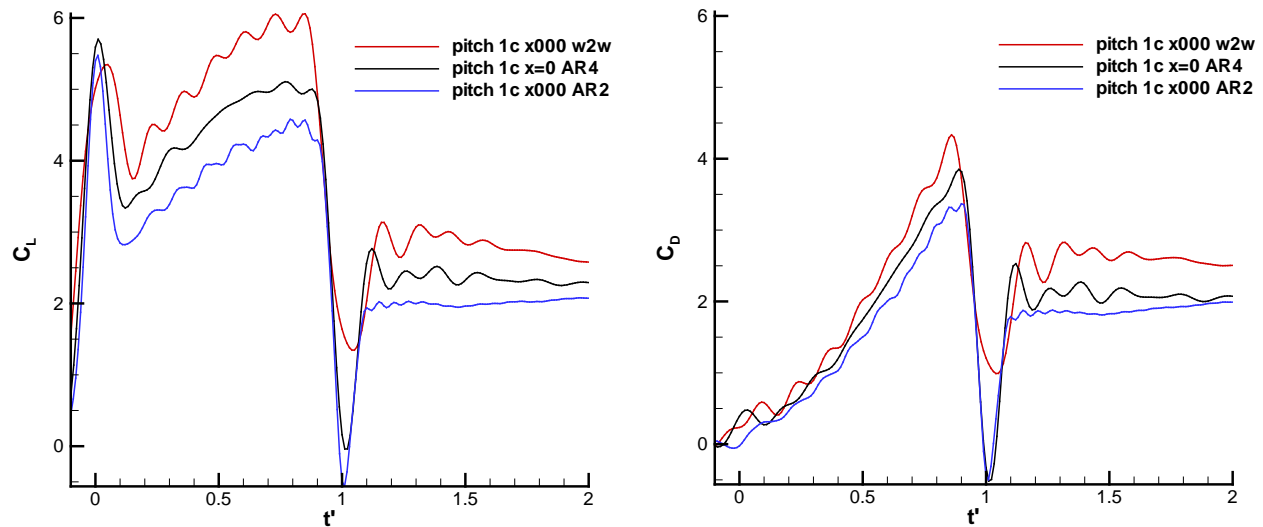
Figure 4. Aspect ratio effects on pure-pitch, pivoting about the leading edge; lift (left) and drag (right), 1c case.

The time at which peak lift (stall) occurs does not appear to be affected by aspect ratio for the fast case in Figure 4, in contradistinction with the slow case in Figure 3. In drag coefficient, aspect ratio differences for both slow and fast cases are more benign than for lift.

We next consider the role of the pitch pivot point, by taking five different pivot point locations: $x/c = 0$, 0.25, 0.5, 0.75 and 1.0; that is, proceeding from the leading to the trailing edge. Figure 5 presents the results for plates of all three aspect ratios for the 1c case, while Figure 6 focuses on the AR=4 plate in the 6c case.

Pivot point effects in Figure 5 parallel aspect ratio effects in Figure 3; that is, (1) difference in lift are more profound than in drag, and (2) differences in circulatory lift are primarily a constant offset in the ordinate, and not a slope change. A more forward pivot point produces higher peak lift, but in all cases, the circulatory lift peaks at about the same time: t'~0.9 at motion cessation. Differences in noncirculatory lift are quite obvious, and are in good agreement with predictions of unsteady airfoil theory (see e.g., McGowan et al.[10]). With the pivot point maximally upstream, there is a positive noncirculatory lift spike when pitch-acceleration is positive (early in the motion history), and a negative spike in both lift and drag when pitch-acceleration is negative (t'~1). For pitch about the midchord, there is no noncirculatory contribution, arguing from symmetry, again in accordance with unsteady airfoil theory. For pitch about a point downstream of the midchord, the sign of the force spike reverses: negative spike in lift when acceleration is positive, positive spike in lift and drag with acceleration is negative. From the aforementioned unsteady airfoil theory, the x/c=0.75 pivot point also has a special attribute; the pitch rate contribution is zero, once again in accord with theory.
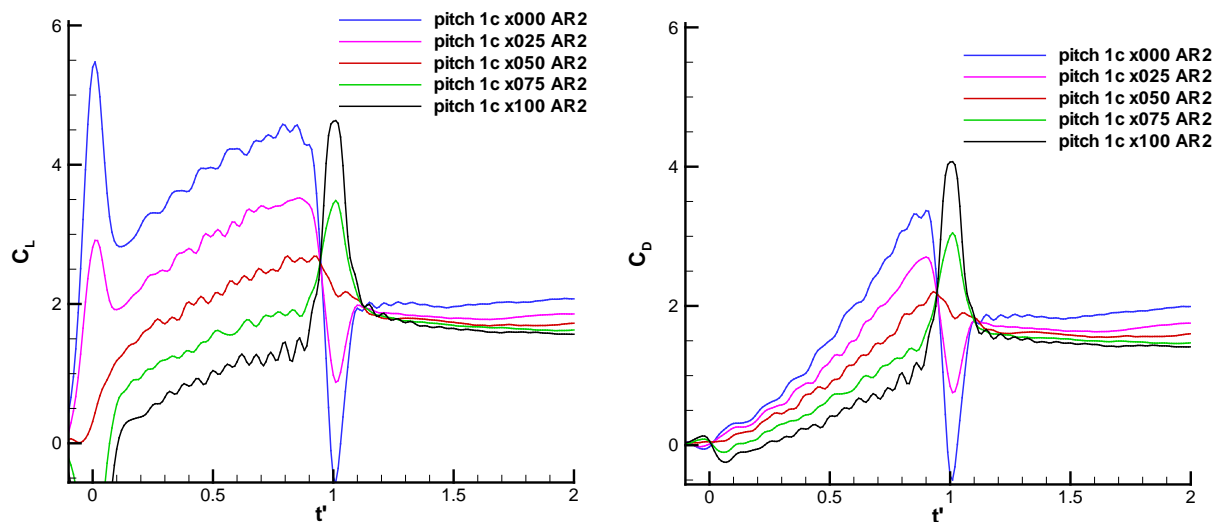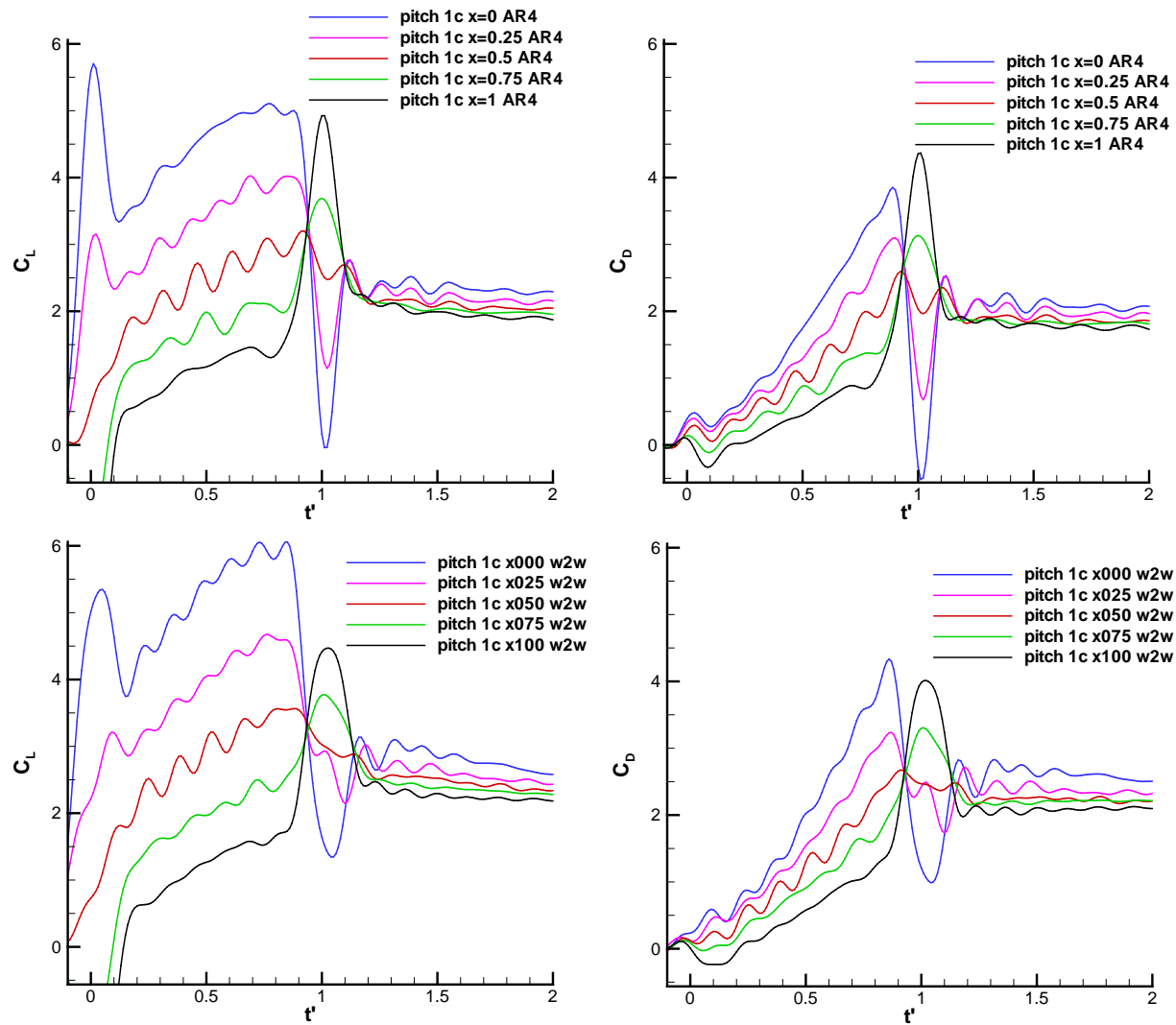
Figure 5. Pivot-point effects for pure-pitch cases, 1c motion, AR=2 (top row), AR=4 (middle row) and nominally 2D (bottom row); lift (left column) and drag (right column). Pivot point at leading edge (x/c = 0), x/c = 0.25, 0.5, 0.75 and 1.0 (trailing edge).

Figure 6 discusses pitch pivot point effects for the slow-case (6c), for the AR=4 plate. As with the fast case (1c, Figure 5), a more upstream pivot point produces higher peak lift due to a constant positive offset. But now the acceleration is too slow to produce a demonstrable noncirculatory force contribution in any of the motions. We mention in passing that peak lift for the x/c = 0 pivot-case appears to occur when t'~4; that is, at a time from motion onset during which the free-stream has traveled approximately 4 chords. The offset between the five lift curves in Figure 6 can be regarded as an offset in the abscissa alternatively as an offset in the ordinate. Considering the former, each curve differs from its neighbor by t'~0.25 – that is, by approximately the difference in pivot point location. Thus in Figure 7, we shift the time-basis of the x/c=0.25 curves by 0.25c forward, the x/c=0.5c curves by 0.5c forward, and so forth. One obtains nearly complete overlap of all five lift curves (agreement is not as good in drag), up through t' ~ 4. It therefore appears that if the pivot point is taken as an origin for counting convective time, in all cases peak lift is achieved when the free-stream has convected downstream through a distance of 4 chords past the pivot point. The subsequent lift troughs and crests originating from vortex shedding events also coincide in convective time. One is tempted to wonder whether this "peak lift event" is coincidental, or relatable to the oft-quoted conceptualization of a critical "formation number" of 4[4].
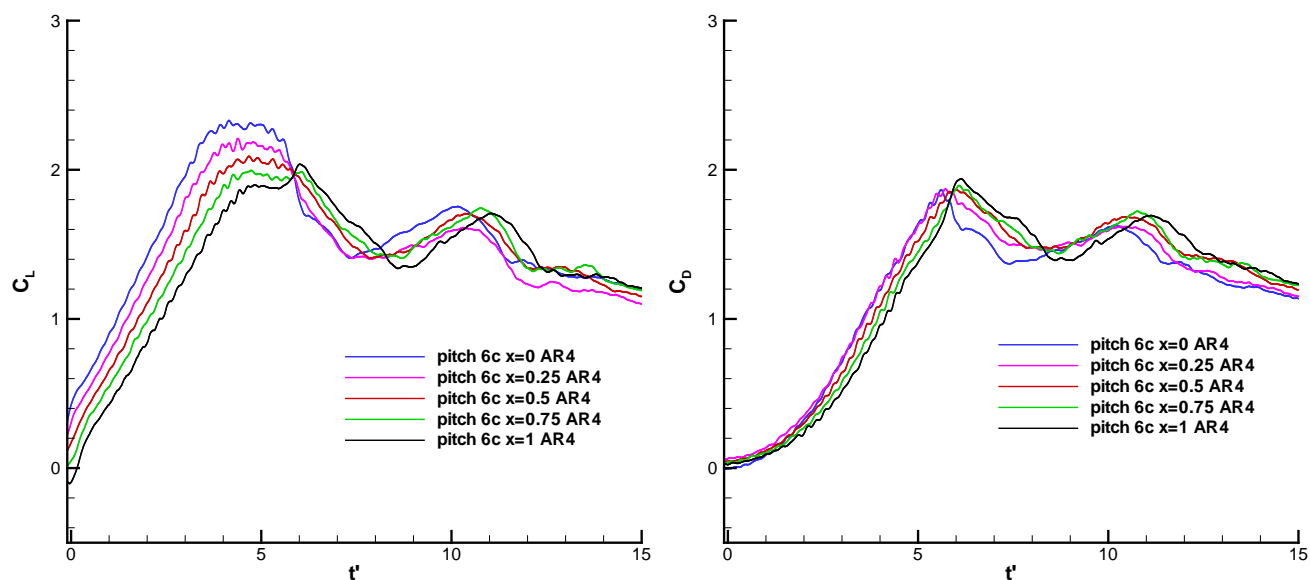
Figure 6. Pivot-point effects for pure-pitch cases, 6c motion, AR=4 only (other aspect ratios are similar). Lift (left column) and drag (right column). Pivot point at leading edge (x/c = 0), x/c = 0.25, 0.5, 0.75 and 1.0 (trailing edge). Moving the pitch pivot point downstream produces a phase-shift (delay in time) and slight decrease in peak lift.
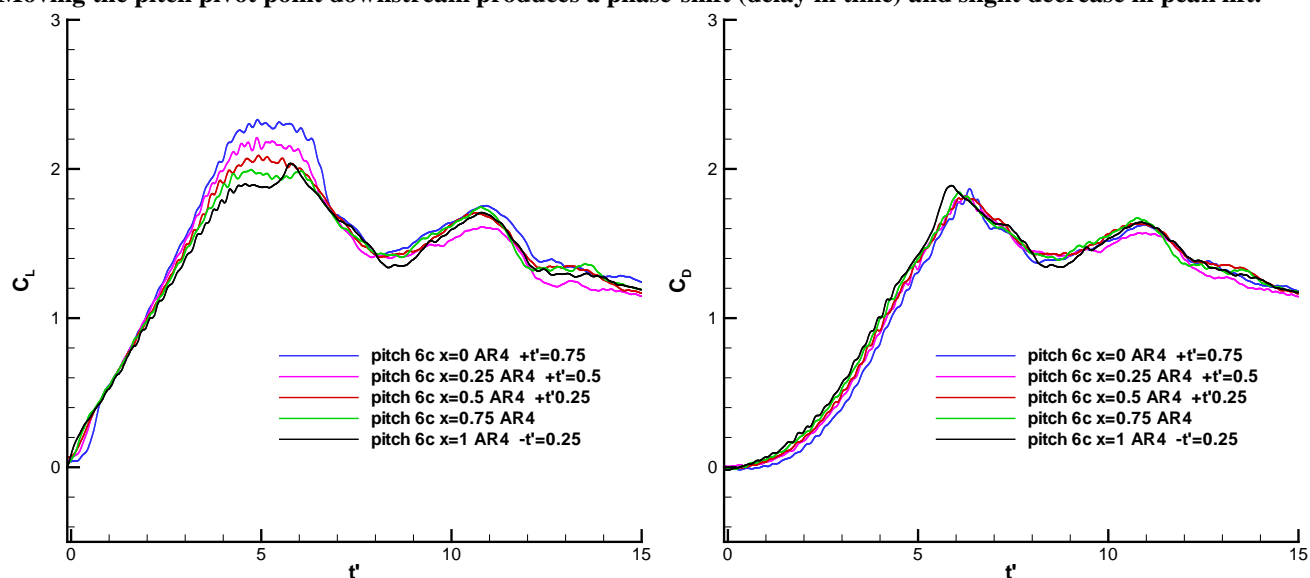

Figure 7. Pivot point effects for pure pitch cases, 6c motion from Figure 6 with lift (left) and drag (right) curves shifted in convective time according to pivot point location.

The case of combined streamwise velocity ramp (surge) and angle of attack ramp (pitch) is shown in Figure 8, for the 1c (fast acceleration) case, for the same five pivot points as in the preceding two figures. Unlike the pitch-ramps with constant relative free-stream speed, there is no noncirculatory aerodynamic force discernable at motion onset since the second derivative of both motion-directions is close to zero. Towards t'~1, the behavior in Figure 8 appears to be much akin to that of Figure 5. The extent to which circulatory lift is similar between Figure 8 and Figure 5 is another way of stating how much flow-history effects matter, between that of the accelerating free-stream and constant free-stream, respectively. If free-stream acceleration effects are slow or are otherwise benign compared to pitch-rate effects towards t'~1, then the two respective sets of lift and drag curves would agree near t'~1. Judgment is subjective, but one may observe that the lift and drag spikes – that is, the noncirculatory effects, which have no flow-memory, are indeed very similar between Figure 5 and Figure 8. For circulatory forces, the comparison is not so clear. But what is clear is that as in Figure 5, moving the pivot point aft results in both lower lift and drag, and the sign and amplitude of the noncirculatory force spikes has the same relation to pivot point location in Figure 5 and Figure 8.
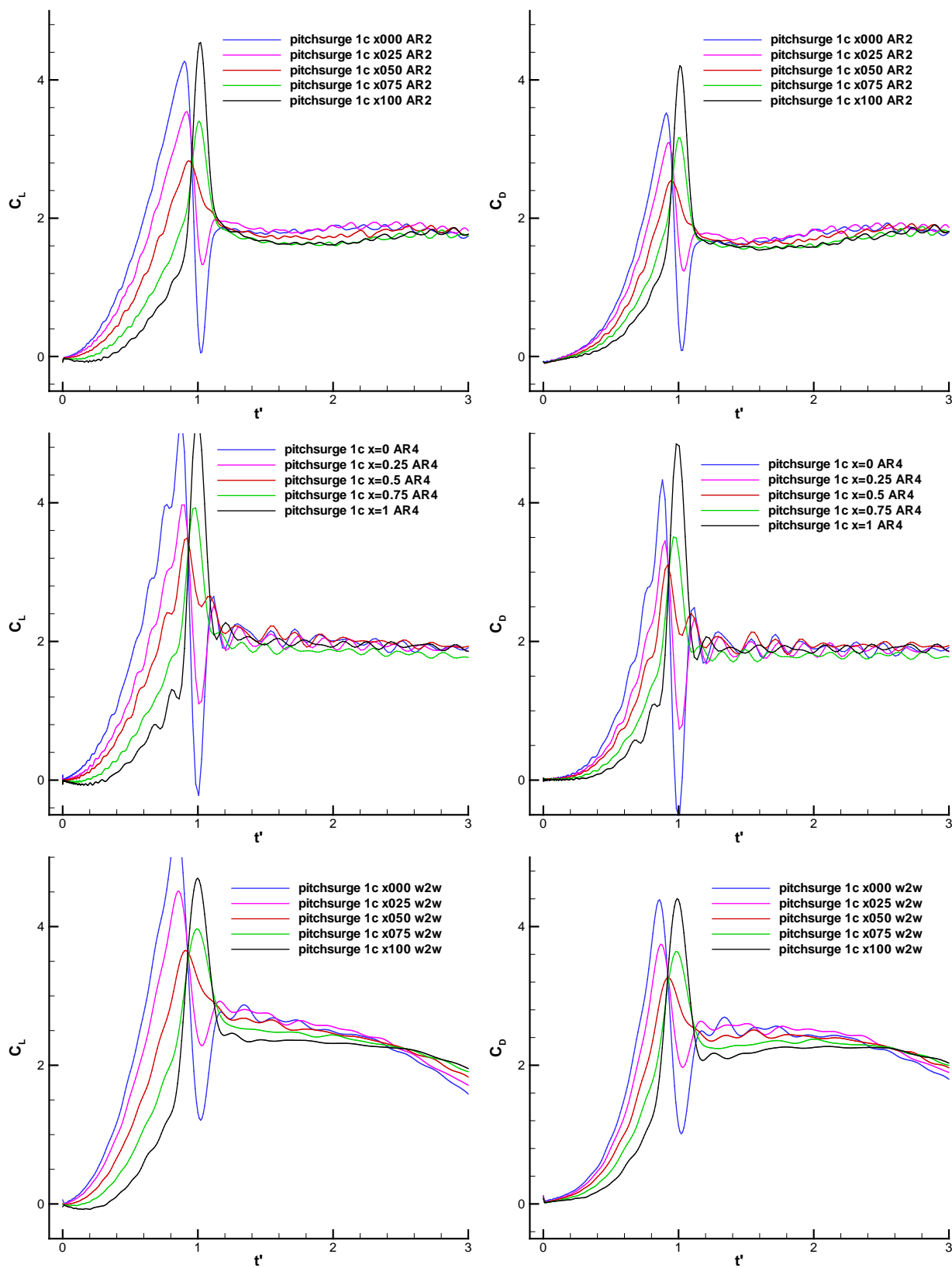
Figure 8. Combined pitching and surging motion, where the plate undergoes a smoothed linear pitch ramp about the pivot point as marked, and simultaneously a smoothed linear ramp in its translational speed. 1c motion, AR=2 (top row), AR=4 (middle row) and nominally 2D (bottom row); lift (left column) and drag (right column). Pivot point at leading edge (x/c = 0), x/c = 0.25, 0.5, 0.75 and 1.0 (trailing edge).

We next turn to a comparison of the three translational motions: pitch ramp, pitch/surge ramp, and surge ramp. Where kinematically possible, a forth motion is added, not heretofore mentioned. This is an "equivalent" plunge, inspired by pitch-plunge comparison by McGowan et al.[10]. For the constant free-stream pitch, one takes the "equivalent" plunge speed from the quasi-steady relation that ratio of plunge speed to free-stream speed equals the instantaneous incidence angle in the purely pitching case. The pitch pivot point effect is neglected, as are the higher derivatives and any wake information as considered by McGowan et al[10]. Plunge lift and drag coefficients are normalized not by dynamic pressure from the free-stream speed, but from the magnitude of vector sum of free-stream speed and plunge-speed. The result for the 1c motion is shown in Figure 9 for the AR=2, 4 and nominally 2D plates for the 1c acceleration, and in Figure 10 for the AR=4 plate for the 6c acceleration. The purely-pitching and the pitching-surging cases are again with respect to a pivot point at the leading edge (x/c = 0).
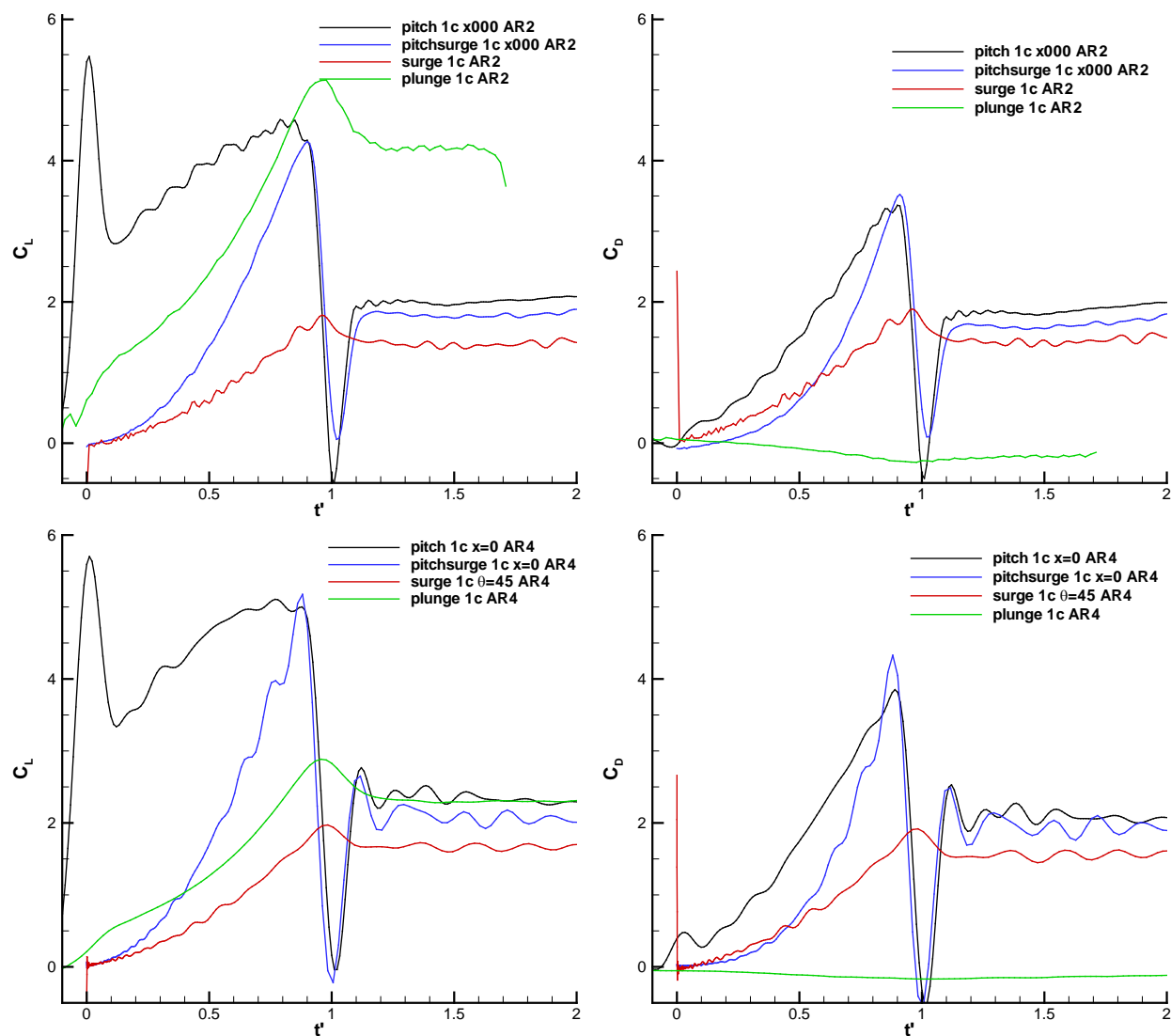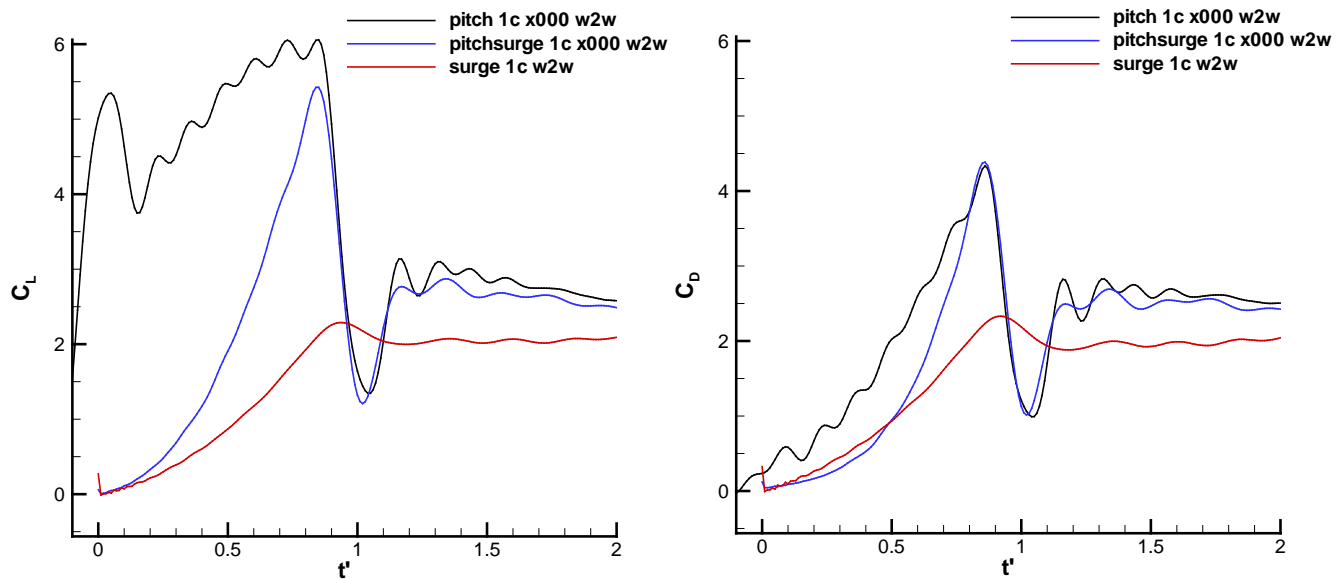
Figure 9. Comparison of pitch ramp, pitch-surge ramp and pure surge-ramp, and "equivalent" plunge: 1c motion, AR=2 (top row), AR=4 (middle row) and nominally 2D (bottom row); lift (left column) and drag (right column). Pivot point is at the leading edge (x/c = 0) for the pitch-ramp and pitch-surge ramp. Plunge force coefficients are non-dimensionalized on total velocity (freestream and plunge velocity) dynamic pressure.
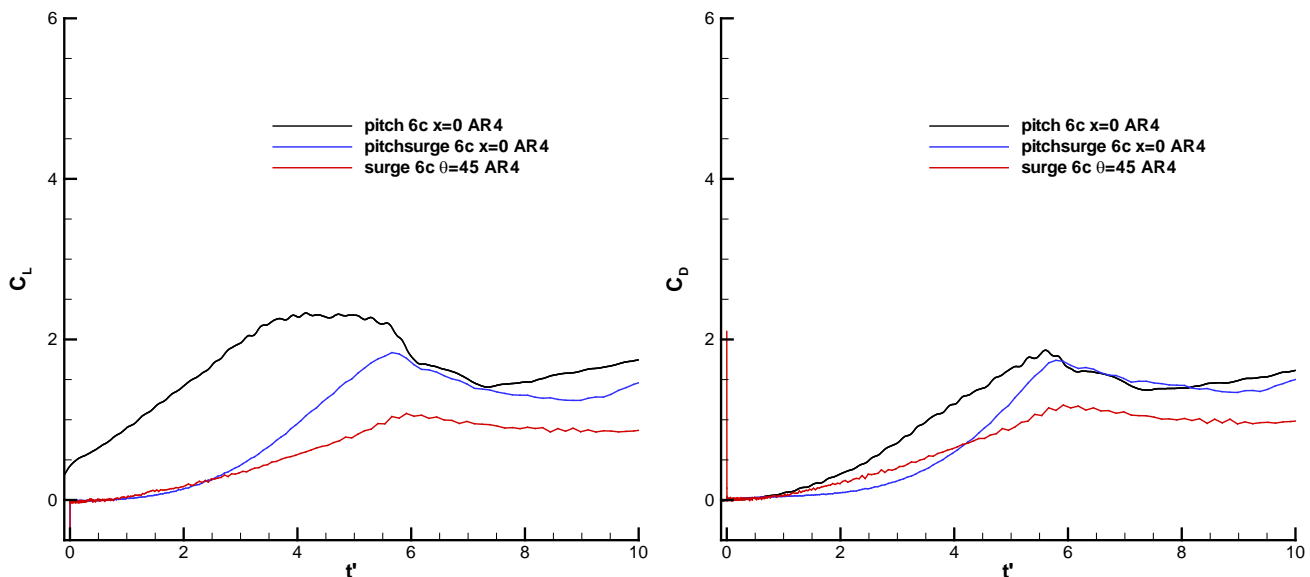

Figure 10. Comparison of pitch ramp, pitch-surge ramp and pure surge-ramp, 6c motion, AR=4 only; lift (left column) and drag (right column). Pivot point is at the leading edge (x/c = 0) for the pitch-ramp and pitch-surge ramp.

In both Figure 9 and Figure 10, the pitching case has much higher lift and drag than does the respective surging case, for every aspect ratio and for both motion rates. The combined pitch-surge ramp is an intermediate case, as is to have been intuitively expected. Early in the motion, (t'~0), it behaves akin to the surging case, with aerodynamic force production attenuated due to low dynamic pressure. As time proceeds, the pitch-surge case comes to approximate the purely pitching case. The plunging case has a lift history somewhere in between that for the pitching and pitch-surge cases, but a drag history altogether different, with drag outright negative, evidently from strong leading-edge suction. Since lift and drag are oriented in the wind axis of the freestream of the water tunnel, there is no pressure force normal to the plate in the drag axis, other than what acts on the leading and trailing edges of the plate. The plunging case, and the pure-surging case, completely lack a noncirculatory lift or drag spike. The noncirculatory forces are based completely on dimensional acceleration and independent of convective nondimensionalization. Since all non pure-pitch motions have constant acceleration with respect to

convective time, the acceleration will be exponentially dependent on time and asymptote to zero at initial condition, thus providing no "added-mass" spike.

As mentioned before, airfoil theory predicts that the pitch-rate contribution will be identically zero if the pivot point is taken at $x/c = 0.75$[10]. Accordingly, Figure 11 compares pitch and pitch-surge with pivot about $x/c = 0.75$, with pure-surge and plunge, all for the AR=4 plate, for the same acceleration profile as in Figure 9 (that is, acceleration over one convective time). Indeed the lift history now compares much better across all four kinds of motion. The pitch case, even with the pitch-rate effect removed, still achieves significant lift during the initial stage over the two non-convective cases. One can intuit that the cause is the nonzero free-stream, allowing for production of leading-edge and trailing-edge vortices immediately at motion onset. The plunge case has also been re-nondimensionalized with respect to the total velocity, which is the magnitude of the vector sum of the freestream velocity and the plunge velocity. The lift is lower than for the pitching case, but still higher than in the non-convective cases. Drag throughout most of the accelerated portion of the motion is nearly identical for the pitch and pure-surge cases, whereas the pitch and pitch-surge cases have nearly equal drag for t' >0.9.

Figure 12 restates the aforementioned results with focus on the pure-surge cases for the three aspect ratios. The nominally 2D plate has slightly higher slope in both lift and drag that for the AR=2 and AR=4 plates, which are mutually similar. The 2D plate also achieves peak lift and drag slightly sooner than the other two plates; that is, at t'~0.9 instead of t'~0.95. Weak aspect-ratio dependency for the surging translational case is consistent with earlier findings for free-to-pivot plates in hover[9], which are akin to a periodic version of the present transient problem.
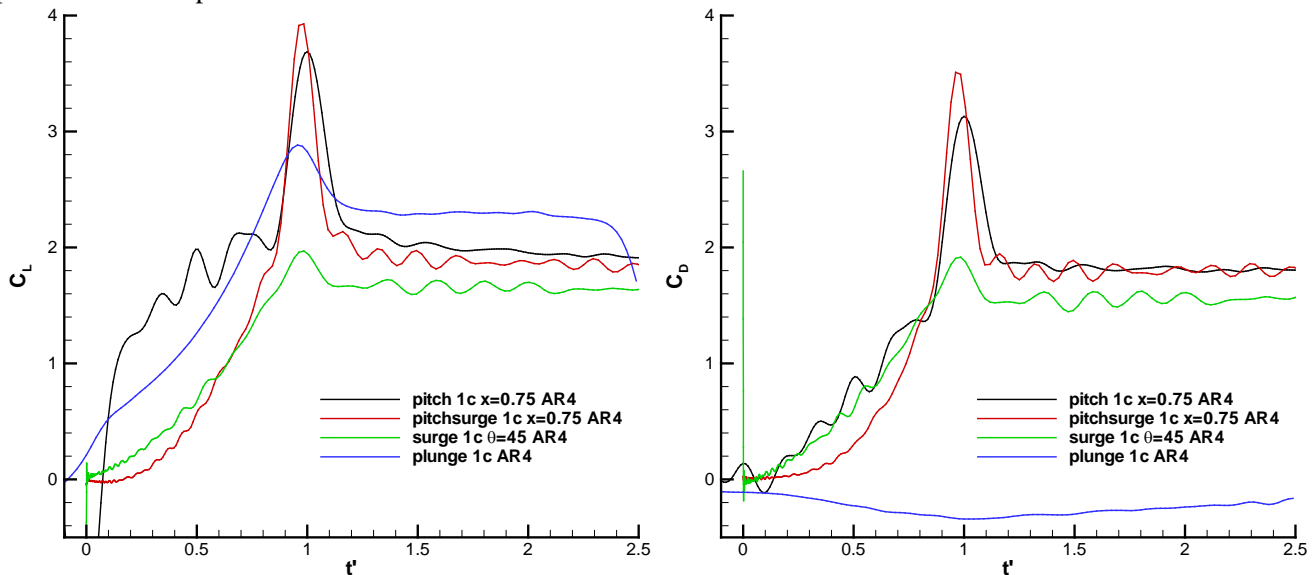

Figure 11. Comparison of pitch and pitch-surge, this time with pivot point at x/c = 0.75; pure surge and plunge motions; lift coefficient (left) and drag coefficient (right). Plunge force coefficients are non-dimensionalized on total velocity (freestream and plunge velocity) dynamic pressure.

It should be mentioned that after a "sufficient" number of convective times after cessation of relative acceleration between the ambient fluid and the plate, all force histories for a given plate geometry and incidence angle should converge to the same steady or oscillatory (if there is Karman shedding) behavior. It is noted from Figure 3 that the AR=2 plate does not exhibit the oscillatory shedding. A sample result containing long time-basis, for the AR=4 plate undergoing acceleration in pitch, pitch-surge and surge, is shown in Figure 13. Indeed, the three cases eventually converge to a lift and drag coefficient of ~1.5, consistent with the accepted result for static flat plates (see for example Hoerner[11])
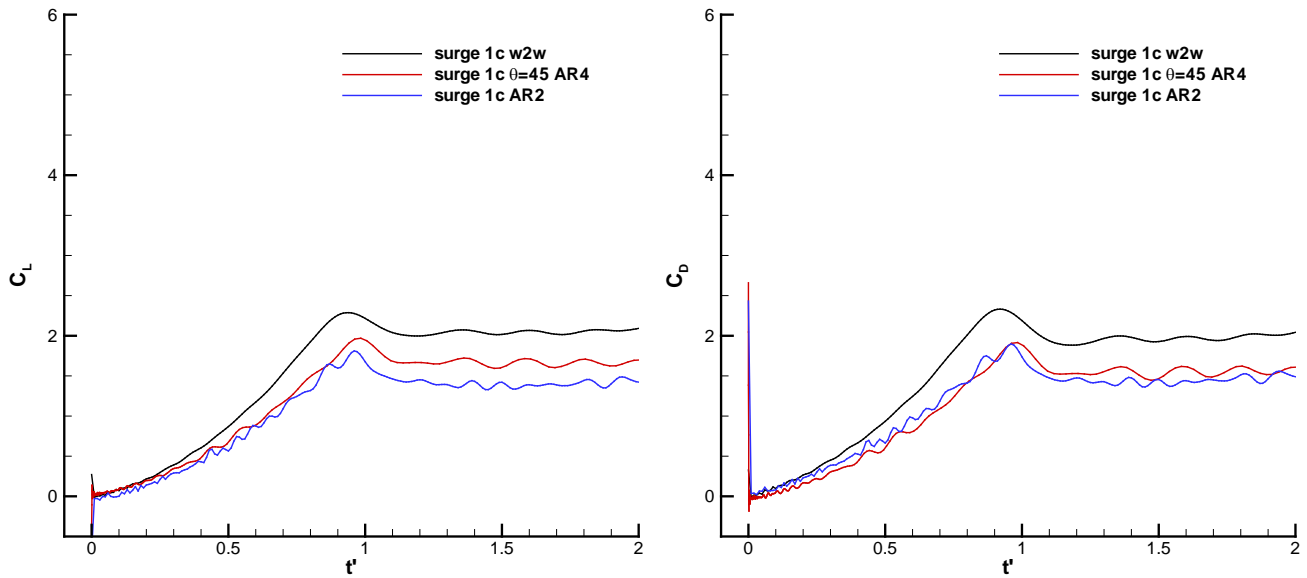
Figure 12. Aspect-ratio effects on surging translational motion (1c streamwise acceleration).
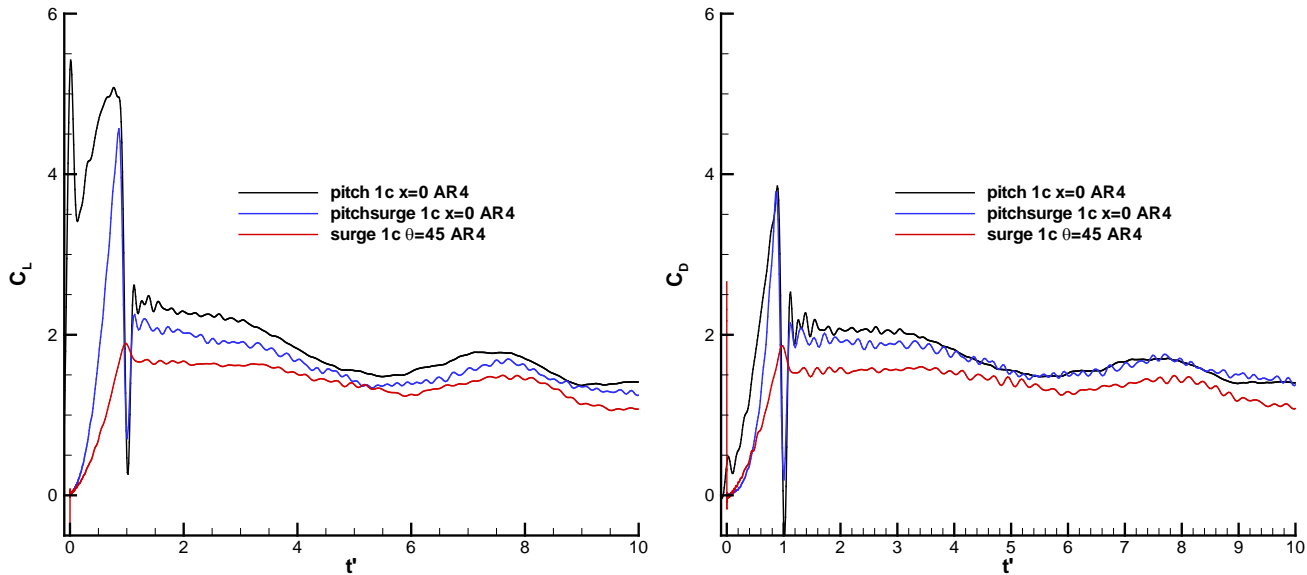

Figure 13. Long-term history of lift and drag for AR=4 1c motions.

Figure 14 presents flow visualization for the 1c translational surge to a Re=10,000 velocity. Both trailing-edge and leading-edge vortices appear to begin formation immediately upon motion startup, and are already obvious by t'=0.5. The trailing edge vortex does not convect with the plate, whence separation between its core and the plate's trailing edge grows with time. The leading edge vortex remains compact and "attached" to the plate through t'=0.5. It visibly lifts off of the plate's suction side by t'=3, en route to disconnecting from its origin at the leading edge and beginning downstream convection in the plate's reference frame.
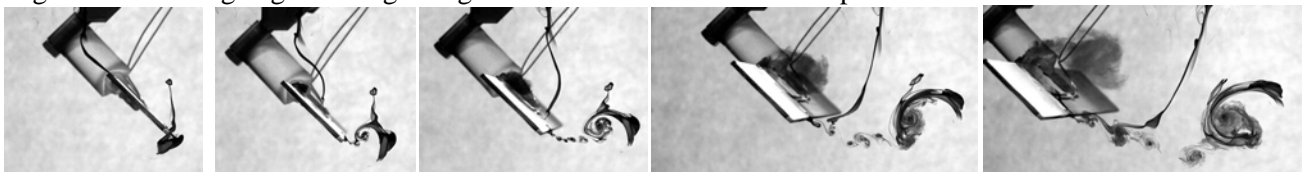

Figure 14. Flow visualization by injection at ¾ span location, leading and trailing edge of AR=4 plate, translational pure-surge with smoothed linear ramp-change of surging speed from rest over 1 chord of travel, 45° incidence, in quiescent water. In going from left to right, snapshots at t'= ~0, 0.5, 1.0, 2.0 and 3.0.

We now turn to comparison between translational surge and rotational surge (Figure 15). In the rotational case, the plate begins at rest and starts to rotate about a point 0.5c inboard of the root, accelerating over 1c to a constant angular velocity. Since the tangential velocity varies radially from root to tip, a reference plane at 1.875c outboard from the point of rotation is used for nondimensionalising velocity and chords traveled.

The rotating plate has an effective doubling of aspect ratio, since it is only one "wing panel", and therefore it is appropriate to compare AR=2 rotation with AR=4 translation. However, since the AR=2 and AR=4 translational surge cases are so similar (Figure 12), pedantry in attempting to define appropriate aspect ratio for the rotating plate is rather moot. Figure 15 compares both lift and drag, showing that the two coefficients have nearly identical histories, of each respective case. If lift and drag for a plate at 45° incidence are so similar, then this suggests that all leading-edge suction is absent at all times, and that pressure-force dominates friction; the total aerodynamic force vector is essentially normal to the plate's leeward side, with a negligible viscous contribution to axial force in the plate's reference frame. Absence of leading edge suction throughout the motion is consistent with the flow visualization in Figure 14, where a leading-edge vortex begins formation immediately upon motion onset. The rotating wing has force coefficient slope persistently lower than that for the translating wing, in both lift and drag, from motion onset to cessation of acceleration. Peak force occurs earlier for the rotating wing, and the force peak itself is much more benign for the rotating than for the translating case. In fact, lift and drag attenuate very slightly after acceleration cessation for the rotational case, and then resume build-up in approaching the post-acceleration steady state. Because the motion rig is limited to a 90-degree arc of rotation, it is not possible to truly compare relaxation to steady-state (or to bluff-body shedding) between the rotating and translating cases. Nevertheless, it is clear that acceleration-induced transients for rotation are lower than for translation. Also, the rotating case appears to have a jump from zero aerodynamic force (both lift and drag) early in the motion, perhaps due to noncirculatory effects.
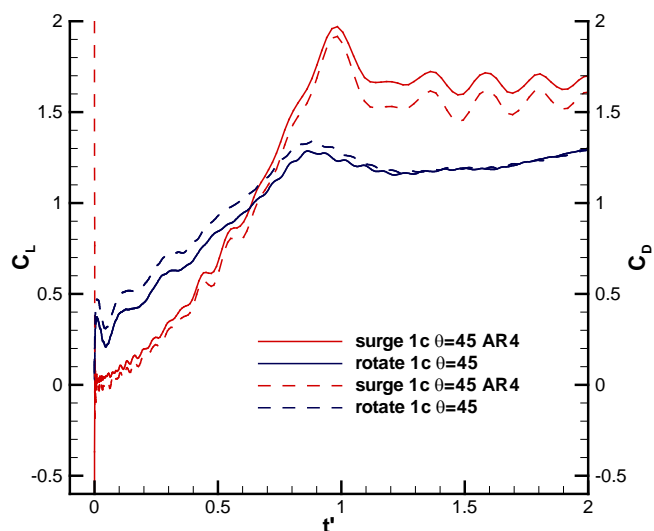

Figure 15. 1c translational vs. rotational motions: AR=4 plate in translational surge (red) and AR=2 plate in rotational surge (black). Lift (solid line) and drag (dashed line). Both motions hold θ =45° constant.

All of the aforementioned results were obtained with water as the working fluid. To study broad dependence on Reynolds number, we now turn to mixtures of glycerin and water, where the kinematic viscosity of the working fluid can easily be varied. As glycerin-water mixtures can not be pumped by the water tunnel's pump, all of the following results were obtained in a secondary tank inserted into the tunnel's test section.

With first consider the translational case. Trends in lift and drag for the AR=4 surging plate accelerating over 1c is shown in Figure 16, with Reynolds number based on eventually-attained relative free-stream varying from ~14 (nearly pure glycerin) to 10,000 ("pure" water). We also compare the experimental results with immersed-boundary-method computations from the University of Florida. In the experiment, kinematic viscosity

is determined by dropping a sphere of known mass and diameter into the working-fluid, noting the terminal velocity and applying known curve-fits for a sphere's drag coefficient vs. Reynolds number (based on diameter)[12].

The essential feature of Figure 16 is that during the accelerated part of the motion, lift is essentially independent of Reynolds number, with the possible exception of the lowest-Re case, Re=14. On the other hand, at later time, after a steady relative free-stream has been established, lift values relax to different steady (or shedding) values, depending on Re, but without a clear trend with Re; that is, it is not the case that lowest Re produces lowest or highest lift. Thus the transients in lift are weakly Re-dependent, or not at all; but the long-term lift history has an unclear trend with Re. The situation with drag has its own quirks. First, unlike the "high" Reynolds number case considered heretofore, lift and drag histories do not resemble each other. For a plate at 45° incidence, this means that the net aerodynamic force is not wall-normal. Second, there is an interesting dependency on drag with Reynolds number: for Re in going from 300 to 14, the drag increases substantially, but in going from 10,000 to 300, there is very little change in drag histories.

Comparison between experiment and computation is muddled by a notable difference between the respective definitions of surge acceleration profile. Computation uses a linear profile with dimensional time, while experiment is linear with non-dimensional time; refer to Figure 2 (b) and (c). There is an obvious difference in the resulting forces during the accelerated part of the motion, but long-time propagation of these effects is unclear, and one might conjecture that by t'~2, flow "memory" of the acceleration profile has relaxed; see for example Jones and Babinsky[13]. With that distinction in mind, drag is underpredicted by computations for low Reynolds number, but all drag curves collapse for Re>100. Trends for lift are a more complicated, as none of the curves tend towards a common grouping at large convective time.

While experimental data cannot segregate pressure-forces from friction-forces, some insight can be gleaned if the coordinate system is rotated by 45° to be aligned with the plate's cross section. Thus one obtains axial and normal force; these are plotted in Figure 17. One finds a strongly increasing axial force with decreasing with Reynolds number. Normal force also increases with decreasing Reynolds number, but the trend is far weaker than for axial force. The experimental force values are again consistently larger than the computational.
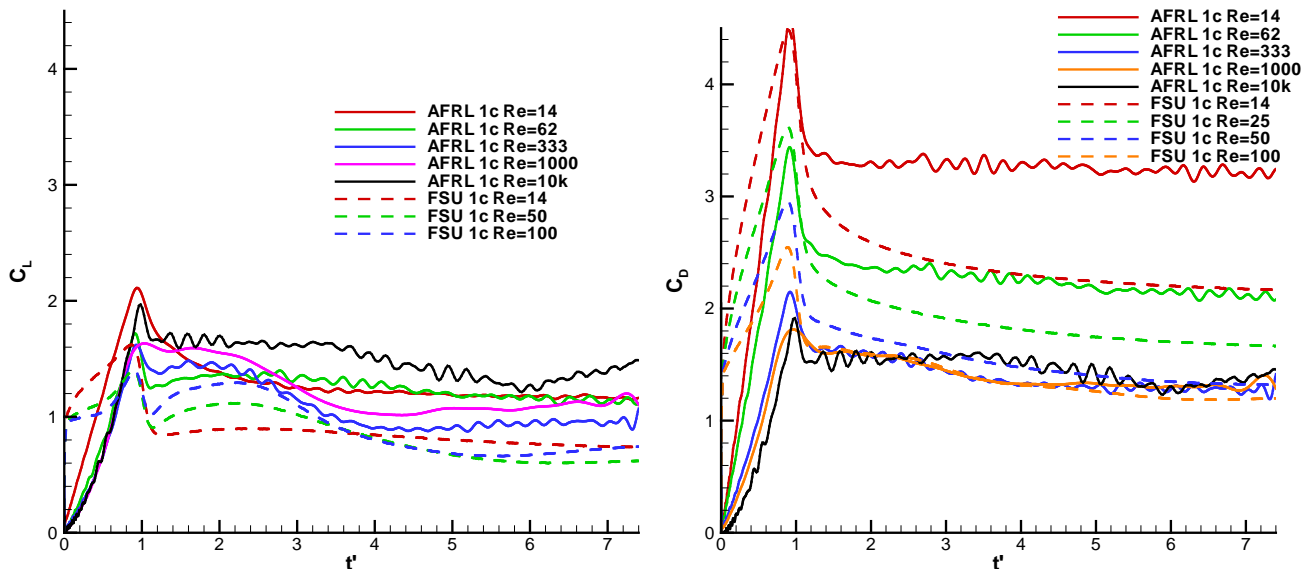

Figure 16. Reynolds number dependence of lift (left) and drag (right) for an AR=4 plate in 1c 45° surge motion. Solid lines are AFRL experiments and dashed lines are FSU computations.
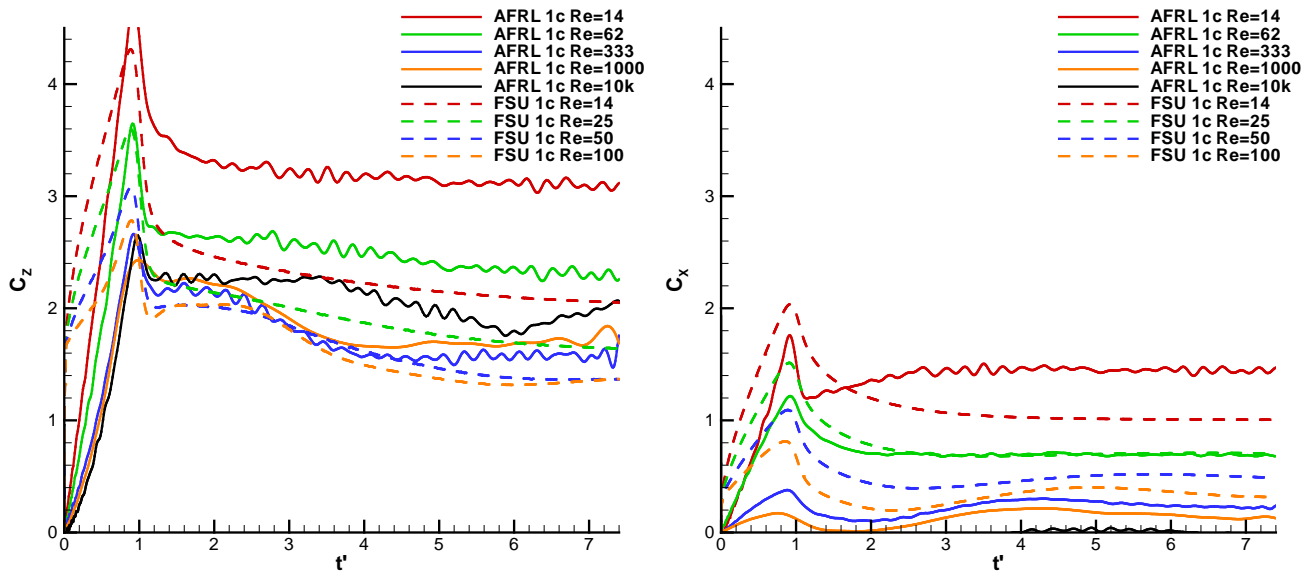
Figure 17. Reynolds number dependence of plate normal (left) and axial (right) coefficients for an AR=4 plate in 1c 45° surge motion. Force coordinate system is rotated 45° from Figure 16.

Figure 18 considers Reynolds number dependency of lift and drag for the AR=2 in rotational surge. Unlike in the translational case, there is an obvious and monotonic dependency of drag on Reynolds number: in all case, the lower the Re, the higher the drag, albeit the trend is strongest at lowest Re, as it was for the translating case. Lift during the accelerated portion of the motion is again Re-independent, but with the exception of the Re=1000 case, lift is also Re-independent in its subsequent history. While we lack in the present study the flowfield elucidation to speculation on what is responsible for the Re-trends in rotational vs. translational motion, it is evident that the rotational-translation comparison in Figure 15 is not as simple at lower Re.
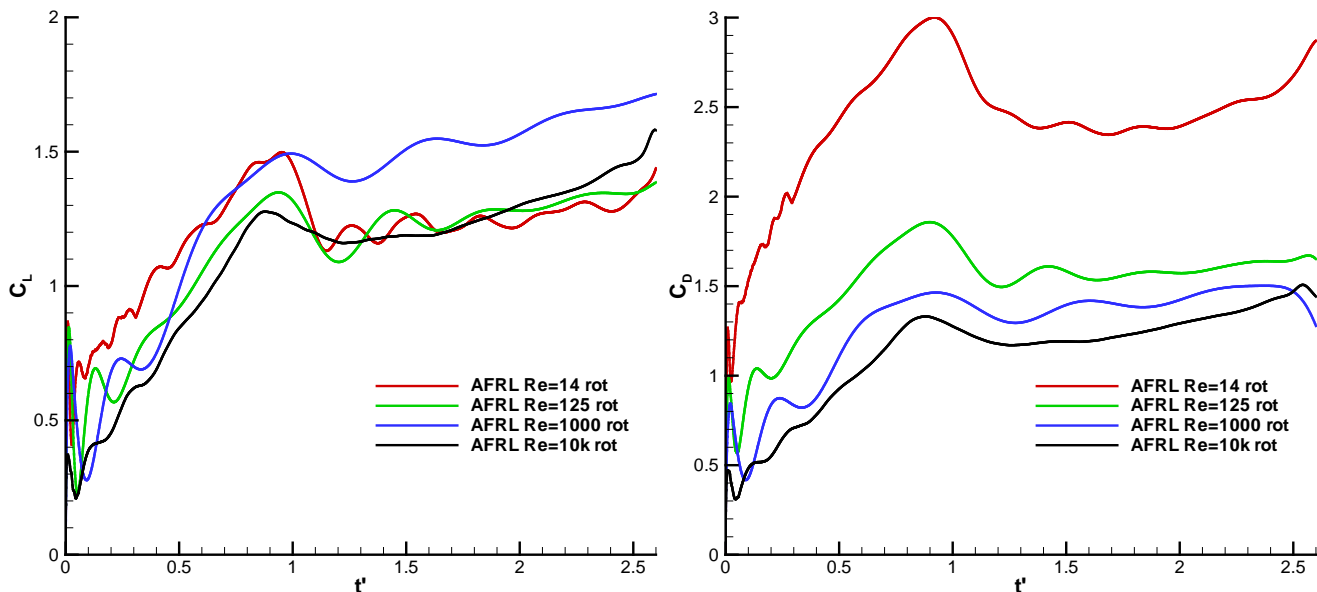

Figure 18. Reynolds number dependence of lift (left) and drag (right) for a rotating AR=2 plate accelerating over 1c.

Conclusion

We considered four routes for a flat plate to pass from zero aerodynamic force to a steady-state condition at 45° incidence, at different motion rates and typologies. The salient issue is comparison of transients in lift and drag before convergence to a common steady-state or oscillatory value. Motions included translational and rotational cases. One variant has the plate at fixed incidence of 45°, undergoing a constant-acceleration over some convective time, either in rotation or translation. This was the only rotational variant, but translational variants included a pure pitch about some prescribed point along the chord, in steady free-stream; a combination of pitch and surging acceleration; and a pure-plunge in steady free-stream. For translational motion, three different aspect ratios were considered: AR=2, 4 and nominally 2D. Rotations were limited to a semi-aspect ratio of 2. Translational or rectilinear pitch produced much higher force coefficients than translational surge, with a discernable trend in force evolution vs. pitch pivot point location in accordance with unsteady airfoil theory. Noncirculatory forces for pitch occur only during nonzero pitch acceleration, while for the surging case they occur everywhere that surge acceleration is not zero; measured spikes in lift and drag were consistent with supposition of the noncirculatory contribution. At Re = 10,000, achieved in pure water, rotational acceleration produced lower force coefficient slope and lower peak loads than did the translational acceleration, but the shape of lift (or drag) force history was similar between the two cases. The net aerodynamic force is essentially wall-normal, implying absence of leading edge suction. At lower Re, achieved in glycerin-water mixtures, rotational and translational cases differed more acutely, and lift history differed from that of drag.

References

[1] Ramesh, K.K., Gopalarathnam, A., OL, M., Granlund, K., and Edwards, J. "Augmentation of Inviscid Airfoil Theory to Predict and Model 2D Unsteady Vortex Dominated Flows". AIAA-2011-3578.

[2] Eldredge, J.D., Toomey, J., and Medina, A. "On the Roles of Chord-Wise Flexibility in a Flapping Wing with Hovering Kinematics". *Journal of Fluid Mechanics*, Vol. 659, pp. 94-115, Sept. 2010.

[3] Lentink, D., and Dickinson, M.H. "Rotational Accelerations Stabilize Leading Edge Vortices on Revolving Fly Wings". J. Exp. Biology, Vol. 212, pp. 2705-2719, 2009.

[4] DeVoria, A., Priyanka, M., and Ringuette, M. "Vortex Formation and Saturation for Low-Aspect-Ratio Rotating Flat Plates at Low Reynolds Number". AIAA-2011-0396

[5] Jones, A., and Babinsky, H. "Unsteady Lift Generation on Rotating Wings at Low Reynolds Numbers". *J. Aircraft*, Vol.47, No.3, pp.1013-1021. 2010

[6] Jones, A., and Schlueter, K. "The Effects of Wall Boundaries on the Flow Field of a Rotating Wing". AIAA 2012-2776.

[7] OL, M. V., Bernal, L., Kang, C.-K., & Shyy, W. (2009). "Shallow and Deep Dynamic Stall for Flapping Low Reynolds number Airfoils". *Experiments in Fluids , 46* (5), 883-901.

[8] Granlund, K., OL, M., and Bernal, L. "Experiments on Pitching Plates: Force and Flowfield Measurements at Low Reynolds Numbers". AIAA – 2011- 0872

[9] Granlund, K., OL, M., Bernal, L., and Kast, S. "Experiments on Free-to-Pivot Hover Motions of Flat Plates". AIAA-2010-4456.

[10] McGowan, G., Granlund, K., OL, M., Gopalarathnam, A., and Edwards, J. "Investigations of Lift-Based Pitch-Plunge Equivalence for Airfoils at Low Reynolds Numbers". *AIAA J.*, Vol. 49, No. 7, pp. 1511-1524, 2011.

[11] Hoerner, S. *Fluid Dynamic Drag*.

[12] White, F. *Viscous Flow*. McGraw-Hill, 2nd Edition, 1991.

[13] Jones, A.R, and Babinsky, H. "Unsteady Lift Generation on Rotating Wings at Low Reynolds Numbers". J. Aircraft, Vol. 47, pp. 1013-1021, 2010.